INSTITUTE OF PHYSICS PUBLISHING NANOTECHNOLOGY
Nanotechnology **14** (2003) 799–802 PII: S0957-4484(03)59508-3

Comparing schemes of displacement detection and subharmonic generation in nanomachined mechanical resonators

Florian W Beil, Laura Pescini, Eva Höhberger, Andreas Kraus, Artur Erbe and Robert H Blick

Center for NanoScience and Sektion Physik, Ludwig-Maximilians-Universität, Geschwister-Scholl-Platz 1, 80539 München, Germany

E-mail: florian.beil@physik.uni-muenchen.de

Received 10 February 2003, in final form 7 April 2003
Published 15 May 2003
Online at stacks.iop.org/Nano/14/799

Abstract
We present measurements on nanomechanical resonators operating in the radio frequency range. We apply a set-up which allows the comparison of two schemes of displacement detection for mechanical resonators, namely conventional power reflection measurements of a probing signal and direct detection by capacitive coupling via a gate electrode. For capacitive detection, we employ a preamplifier, mounted close to the sample and connected to it via bond wires, which enables direct measurements of the resonator's displacement. We observe that the response of the mechanical resonator depends on the detection technique applied, which is verified in model calculations. We show results for the detection of subharmonics.

(Some figures in this article are in colour only in the electronic version)

1. Introduction

Nanoelectromechanical systems (NEMS) promise to be extremely fast and sensitive tools for sensor and communication technology and may also be regarded as 'quantum-mechanical' resonators when operated at several gigahertz and ultra low temperatures. Here, we want to present a detailed investigation of two different detection schemes important for achieving sensitive displacement detection in NEMS. This is not only beneficial for communication electronics or scanning probe microscopy, but also for attaining a handle on quantum squeezing experiments with these mesoscopic mechanical systems [1]. After touching on the fabrication of the nanomechanical devices, we will focus on conventional reflection measurements and a detailed comparison to direct displacement detection via a preamplifier will be drawn. This scheme of detection is also suited for probing quadrature squeezed states [2]. Finally, we present results on the generation of sub- and ultra-harmonics in simple beam resonators.

2. Experimental methods

The suspended silicon beams are machined from silicon-on-insulator materials, covered by a 50–100 nm thick metal layer. Electrodes are placed close to these, allowing capacitive excitation and detection (see [3] for details). A scanning electron micrograph of such a structure is shown in figure 1. The details of the techniques used to fabricate nanoscale devices have been reported in more detail in previous work [4–7]. The resonators are driven via the Lorentz force generated by placing the structures in an external dc magnetic field and driving an alternating current along the conducting metal on top of the beams (magnetomotive excitation). The conventional way of detecting the resulting displacement of the oscillating motion is to take advantage of the amplitude dependent impedance $\hat{Z}_{\mathrm{res}}$ of the resonator. The total impedance of the beam resonator in a magnetic field B under harmonic excitation at the eigenfrequency $\omega_0 = 2\pi f_0$ is given as

$$\hat{Z}_{\mathrm{res}}(\omega = \omega_0) = R + \frac{L^2 B^2}{2\mu m_{\mathrm{eff}}}, \tag{1}$$

where ω is the frequency, R the dc resistance, m_{eff} the effective mass of the beam, μ the attenuation constant and L is defined via the length of the beam l as $L = l\frac{\pi}{2}$. Commonly the total dc resistance of the samples is of the order of 40–50 Ω. The change in impedance is detected by tracing the reflected power using a network analyser in combination with a scattering

parameter test set (see figure 1). It should be noted that, depending on the sample's resistance and its matching to 50 Ω, the resonance is observed as a peak, while for other resonances a dip is found. If $R < 50\ \Omega$ than $\hat{Z}_{\rm res}$ is shifted closer to 50 Ω in resonance and a dip is observed, as the lower impedance mismatch means lower reflected power. On the other hand the resonance is observed as a peak if $R > 50\ \Omega$.

Direct displacement detection is enabled by the aforementioned gates. The resonator is driven by an induced Lorentz force, which modulates the capacitance between the resonator and the gates due to the displacement of the beam. This change in capacitance induces the measured voltage signal at resonance $\delta C_{\rm res} \sim \delta V_{\rm res}$. Low-temperature amplification of the small voltage signal is desirable, therefore we use a fast preamplifier (Fujitsu FHX35X) for this measurement. The transistor in general serves as an impedance converter. The set-up and the amplifier are shown in figures 1(b) and (c). As seen the large input impedance has to be accounted for by placing in parallel a resistor of 10 MΩ, a capacitor on the supply line of 47 nF, and an additional resistor of 1.5 kΩ on the output. Due to the gigahertz bandwidth of the HEMT we are able to monitor the charge on the gates with a time resolution in the nanosecond range. A limitation of this set-up is given by the low gain and the still large input capacitance of the circuit. However, a gain increase can be achieved by adjusting the circuit, while the input capacitance can easily be reduced by a further length reduction of the bond wire connecting the gate and amplifier input port.

3. Results and discussion

Several resonators with different dimensions [$(4.8 \times 0.17 \times 0.19)\ \mu\mathrm{m}^3$, $(5.0 \times 0.25 \times 0.19)\ \mu\mathrm{m}^3$, and $(1.2 \times 0.1 \times 0.1)\ \mu\mathrm{m}^3$] were investigated: in figure 2(a) the reflectance spectrum for a magnetomotively driven beam is shown. This resonator possesses an eigenfrequency of 81.7 MHz at 4.2 K. The magnetic field was oriented perpendicular to the beam yet parallel to the sample surface. It has to be noted that this is a hybrid resonator, i.e. the combined elastic constants of Au and Si will determine the response. The inset in figure 2(a) shows nonlinear effects, seen in a typical hysteresis [5]. The eigenfrequency can be tuned by electrostatic forces exerted on the beam when applying a dc voltage $V_{\rm g}$ at the electrodes depicted in figure 1(a). As expected, we find the shift in eigenfrequency Δf_0 to be dependent on the gate voltage as $\Delta f_0 \sim V_{\rm g}^2$.

Using capacitive detection on an identical resonator for probing the mechanical resonances leads to the traces depicted in figure 2(b). By evaluation of the full width at half maximum δf_0 we observed an enhanced quality factor of $\Gamma_{\rm cap} = f_0/\delta f_0 = \omega_0/\delta\omega_0 \simeq 4100$ as compared with figure 2(a). This value is increased by a factor of 1.50, which can be explained in the following way: the maximum induced voltage over the beam due to its motion in the magnetic field can be written as

$$V_{\rm ind}(\omega) = \mathrm{i}\omega L B \epsilon A(\omega), \tag{2}$$

where ϵ denotes a mode-specific factor and A the amplitude of the oscillation. This approach is justified if a periodic motion

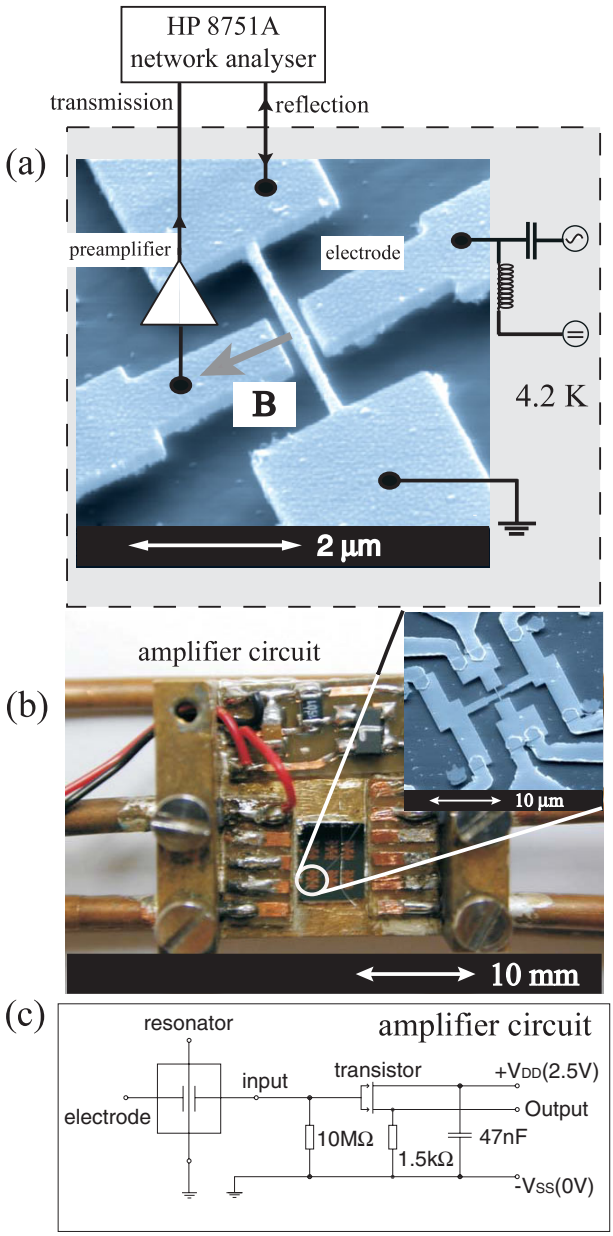

Figure 1. (a) Scanning electron micrograph of one of the nanomechanical resonators: the silicon beam is covered by a thin Au layer, the left and right electrodes allow application of an additional dc voltage to tune the eigenfrequency or an ac voltage for driving purposes. Also pictured is the experimental set-up for sampling the mechanical properties of the suspended beam. For characterization we employ a network analyser. (b) Preamplifier: one of the gates is coupled to the amplifier enabling capacitive detection of the beam's displacement. A magnified view of one structure is depicted in the inset. (c) Circuit diagram of the set-up (see text for details).

at frequency ω is assumed. In the following we simply use for $A(\omega)$ a Lorentzian

$$A(\omega) = \frac{1}{\sqrt{(\omega_0^2 - \omega^2)^2 + 4\mu^2\omega^2}}. \tag{3}$$

In order to derive an equation for the case of capacitive detection corresponding to equation (2), it is advantageous to use an expansion to the second order of the capacitance

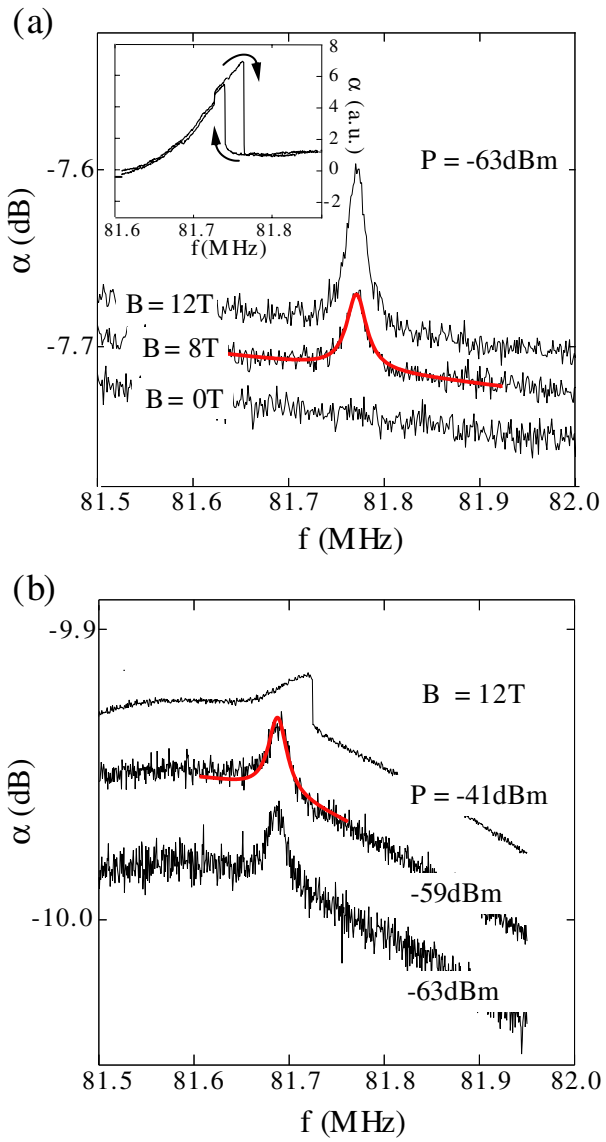

Figure 2. (a) Measured resonances for an incident power of $P = -63$ dBm for increasing magnetic field strength. This mechanical resonator is 4.8 μm long, 170 nm wide and 190 nm thick. The magnetic field is oriented in plane of the sample surface and perpendicular to the beam. By fitting the peak with a Lorentzian we get $f_0 = 81.77$ MHz and $\delta f_0 = 29.84$ kHz. The inset shows the observed hysteresis which emerges when tracing the frequency from low to high (and vice versa) in direct reflection. (b) Resonances in the spectrum detected by capacitive coupling via the preamplifier. The incident power was raised from $P = -63$ to -41 dBm. Values determined for the eigenfrequency and full width at half maximum are $f_0 = 81.69$ MHz and $\delta f_0 = 19.89$ kHz.

between the gate and beam [5]

$$C(A) = C(0) + \left.\frac{\partial C(A)}{\partial A}\right|_0 A + \frac{1}{2}\left.\frac{\partial^2 C(A)}{\partial A^2}\right|_0 A^2 + \cdots. \quad (4)$$

In equilibrium the beam is in a state of minimum total energy. Neglecting contributions from built-in mechanical stresses the electrostatic energy is minimal, the first derivative of $C(A)$ with respect to the amplitude A has to vanish $(\partial C(A)/\partial A)|_0 = 0$. Hence, the induced voltage can be written, using equation (4), as

$$V_{\mathrm{cap}}(\omega) = \frac{Q}{C(A)} \simeq \frac{Q_C}{C_0} - \frac{1}{2}\frac{Q_C}{C_0^2}\left.\frac{\partial^2 C}{\partial A^2}\right|_0 A(\omega)^2$$
$$= V_0 - \frac{1}{2}\frac{Q_C}{C_0^2} C_0'' A(\omega)^2, \quad (5)$$

where C_0'' denotes the second derivative of the capacitance at $A = 0$. Q_C is the accumulated charge on the gate when a potential V_0 is applied to it. The different functional forms of equations (2), (5) result in two observable phenomena:

(1) Capacitive detection leads to a shift of the resonance frequency by $\Delta\omega = \omega_0 - \sqrt{\omega_0^2 - 2\mu^2}$.
(2) Instead of $V_{\mathrm{ind}} \sim A$, we find for capacitive detection $V_{\mathrm{cap}} \sim A^2$ and thus a width reduction of the resonance.

The ratio of the quality factors $\Lambda = \Gamma_{\mathrm{cap}}/\Gamma_{\mathrm{ind}}$ can be written as a function of the resonance frequency ω_0 and of the effective attenuation constant μ. Fitting the reflectance spectrum for magnetomotive excitation with a Lorentzian yields $\mu = 94.2 \times 10^3$ s^{-1}, and we obtain $\Lambda = 1.55$, which agrees very well with the measured value of 1.50. The observed shift of the resonance shows the proper sign, while the absolute value of about 100 kHz is one order of magnitude above the calculated value. We can conclude that capacitive detection probes Γ values larger than the base frequency by a factor of $\sim\sqrt{2}$.

This can also be quantified by representing the sensitivity of a mechanical lever by the minimum detectable force. As shown by Stowe *et al* [8] this force for rectangular levers is limited by vibrational noise and given for a bandwidth of $\mathcal{B} = 1$ Hz by

$$F_{\mathrm{min}} = \sqrt{\frac{2\kappa k_{\mathrm{B}} T}{\pi \Gamma f_0}} \simeq \sqrt{\frac{w t^2 k_{\mathrm{B}} T}{l\Gamma}\sqrt{E\rho}}, \quad (6)$$

where κ is the spring constant of the beam, w, t and l are the width, thickness and length of the beam, E is Young's modulus, ρ the density and k_{B} Boltzmann's constant. Obviously, the aim is to achieve a considerable size reduction of the structures leading to increased eigenfrequencies of the mechanical systems, while another approach is to enhance the Γ value. Capacitive coupling between gate electrode and the metallized resonator is estimated to be 200 aF [9], which translates, at an excitation power of -42 dBm, into a force sensitivity of 9.4×10^{-14} N Hz$^{-1/2}$. Using the set-up discussed above as an electrometer we find a charge sensitivity of 1.3×10^{-3} e Hz$^{-1/2}$, which is two orders of magnitude better than previously measured [10]. Since the network analyser records amplitude and phase of the reflected signal it is also possible to implement a more sensitive lock-in technique for detection.

Yet another approach to increase the sensitivity of the mechanical resonators is given by probing sub- and ultraharmonics of the mechanical motion. In general these harmonics are nonlinear phenomena: the stationary forced oscillation of a linear oscillator follows the frequency of the exciting force, whereas nonlinear oscillators may show resonances at frequencies different from that of the exciting force. In figure 3 we present measurements for two further resonators with modified dimensions of (5.0 × 0.25 ×

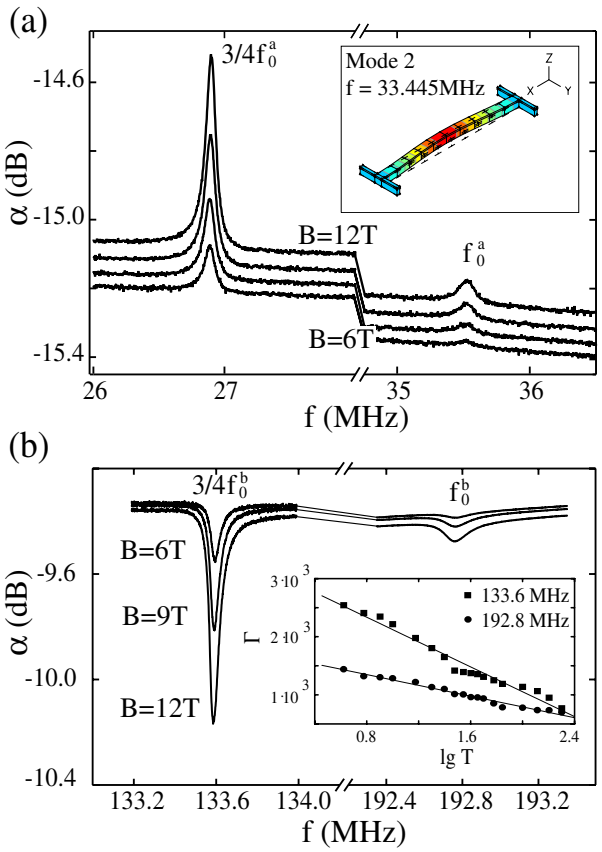

Figure 3. Radio frequency spectrum of the reflected power for two different resonators: (a) the resonance at $f_0^a = 35.5$ MHz can be assigned to the first resonant mode of the beam, while the resonance at 26.9 MHz can be explained by subharmonic excitation at $(3/4)\,f_0^a$. The inset shows a finite-element simulation of an excited mode. (b) Shown is the resonance of the base frequency $f_0^b = 133.6$ MHz and an ultra-harmonic at $(3/2)\,f_0^b$. In the inset the variation of the Γ value with temperature for the two peaks observed is shown. The full squares refer to the resonance at 133.6 MHz while the full circles refer to the 192.8 MHz peak.

0.19) μm^3 and $(1.2 \times 0.1 \times 0.1)$ μm^3. The magnetic field was oriented perpendicular to the sample surface so that an in-plane displacement of the beams is achieved. The measured reflectance spectrum for the first beam in figure 3(a) shows two resonances at 26.9 and 35.5 MHz, whereas the spectrum for the second geometry in figure 3(b) shows resonances at 133.6 and 192.8 MHz. Using finite-element calculations [11] we can assign the resonances at $f_0^a = 35.5$ MHz and $f_0^b = 133.6$ MHz to the first in-plane transverse modes of the resonators. In figure 3(a) the resonance at 26.9 MHz relates to a resonant excitation of a subharmonic at $f_{\rm sub}^a = (3/4)\,f_0^a$ [12]. The amplitude of the resonance measured depends on the form of the excited mode and drops with increasing eigenfrequencies [13], which explains the higher amplitude for the low-frequency subharmonic in figure 3(a). For the second device the resonance at 192.8 MHz can be assigned to resonant excitation of an ultraharmonic at $f_{\rm ultra}^b = (3/2)\,f_0^b$ [12]. These harmonics are due to the nonlinearity of the restoring force introduced by the clamping points of the beams. Following classic experiments on relaxation in crystalline specimens we measured the Γ value over a range of temperatures. Each relaxation mechanism is characterized by its temperature-dependent relaxation rate τ, which in most cases follows the Arrhenius equation [14]. The contribution of each friction mechanism to the internal damping is maximal when $\omega_0\tau = 1$, which results in a peak-like relaxation spectrum when scanning the temperature. The insets of figure 3(b) shows the Γ values of the f_0^b and $(3/4)\,f_0^b$ resonances from 4–200 K. The linear behaviour is indicative of a distribution of relaxation rates rather than the occurrence of one single relaxation mechanism, e.g. related to surface defects, which otherwise might cause a nonlinear response.

4. Conclusion

In conclusion, we have presented measurements on several nanomachined resonators operating in the radio frequency regime. A preamplifier mounted close to the sample enables us to directly detect the displacement of the nanowires by capacitive coupling. This is compared to the conventional method which monitors the reflection of incident power. We find changes in the Γ-factors depending on the detection scheme applied leading to an increase in sensitivity. We also found evidence for the generation of sub- and ultra-harmonic resonances. This will allow to further increase the force sensitivity by pumping the nanomechanical system on the fundamental mode, while probing capacitively on the harmonics for application in quantum non-demolition measurements [2].

Acknowledgments

We like to thank J P Kotthaus and M L Roukes for detailed discussions. We acknowledge financial support from the Deutsche Forschungsgemeinschaft (DFG) under contracts Bl-487/1,2,3.

References

[1] Hu X and Nori F 1996 *Phys. Rev.* B **53** 2419
[2] Rugar D and Grütter P 1991 *Phys. Rev. Lett.* **67** 699
[3] Erbe A, Weiss Ch, Zwerger W and Blick R H 2001 *Phys. Rev. Lett.* **87** 096106
[4] Carr D W, Evoy S, Sekaric L, Craighead H G and Parpia J M 1999 *Appl. Phys. Lett.* **75** 920
[5] Krömmer H, Erbe A, Tilke A, Manus S M and Blick R H 2000 *Europhys. Lett.* **50** 101
Yurke B, Greywall D S, Pargellis A N and Busch P A 1995 *Phys. Rev.* A **51** 4211
[6] Pescini L, Tilke A, Blick R H, Lorenz H, Kotthaus J P, Eberhardt W and Kern D 1999 *Nanotechnology* **10** 418
[7] Kraus A, Erbe A and Blick R H 2000 *Nanotechnology* **11** 165
[8] Stowe T D, Yasumura K, Kenny T W, Botkin D, Wago K and Rugar D 1997 *Appl. Phys. Lett.* **71** 288
[9] MAFIA 1994 *Finite Element Electromagnetic Analysis and Design* ver. 3.20 (Germany: CST GmbH)
[10] Cleland A N and Roukes M L 1998 *Nature* **392** 160
[11] SOLVIA 1997 *Finite Element System* ver. 95.0 (Sweden: SOLVIA Engineering AB)
[12] Kneubühl F K 1997 *Oscillations and Waves* (Heidelberg: Springer)
[13] Ekinic K L, Yang Y T, Huang X M H and Roukes M L 2002 *Appl. Phys. Lett.* **81** 2253
[14] Nowcik A S and Berry B S 1972 *Anelastic Relaxation in Crystalline Solids* (New York: Academic)